Cation and proton exchange, pH variations, and carbonate reactions in a freshening aquifer

C. A. J. Appelo

Faculty of Earth Sciences, Free University, Amsterdam, Netherlands

Abstract. Freshening of aquifers is accompanied by sequential elution of the saltwater (seawater) cations from the sediment's exchange complex. The resulting chromatographic patterns are modeled with a one-dimensional geochemical transport model that can handle the complex interplay of transport and mineral and ion exchange equilibria. The transport part is based on the mixing cell approach, with different time steps for advective and diffusive transport used when required by small grid size. The chemical reactions are calculated explicitly after each time step with the geochemical model PHREEQE. Ion exchange is included in the form of association half reactions, which allows simulation of the dynamic nature of the exchange process. The variation in the constant for proton association is obviated with an activity coefficient for H-X that is derived from the constant capacitance model. All coefficients for the exchange model are obtained by fitting to literature data to be able to perform the modeling as realistically as possible. The code is applied to a laboratory column experiment, and subsequently used to demonstrate chromatographic development of solute profiles in a freshening aquifer. Sequential peaks of Mg^{2+}, K^+, and Na^+ along a flow path in the Aquia aquifer in Maryland are modeled, and the results confirm that the variation of water qualities in this aquifer has basically a chromatographic origin. Proton exchange acts here as a source of acid in $NaHCO_3$ water in which calcite dissolves. This explains the Na^+ to HCO_3^- ratio and high $\delta^{13}C$ observed in these waters.

Introduction

It is well known that the displacement of seawater by freshwater in an aquifer is manifested by a $NaHCO_3$ type water [*Foster*, 1950; *Back*, 1966; *Lawrence et al.*, 1976; *Chapelle and Knobel*, 1983; *Beekman*, 1991; *Stuyfzand*, 1993]. The underlying process is cation exchange, whereby Ca^{2+} from fresh $Ca(HCO_3)_2$ type water exchanges with Na^+ that is present in the saltwater cation exchange complex of the aquifer. The anion HCO_3^- is not affected because natural sediments behave as cation exchangers at the usual near-neutral pH of groundwater. The cation composition of seawater is dominated by Na^+, and Na^+ is therefore an important cation in the seawater exchange complex. However, Mg^{2+} and K^+ are also present at increased levels compared with fresh $Ca(HCO_3)_2$ waters, and these cations reside in the exchange complex at increased concentrations as well. Freshening of an aquifer with a $Ca(HCO_3)_2$ type water requires removal of these increased concentrations. The displacement leads to a chromatographic sequence in which the excess cations are flushed in the order of increasing affinity, i.e., the most selected cation disappears last from the exchanger.

The principles of chromatography are known [*Helfferich and Klein*, 1970] and are addressed regularly in the hydrogeological literature [*Pope et al.*, 1978; *Valocchi et al.*, 1981; *Walsh et al.*, 1984; *Charbeneau*, 1988; *Friedly and Rubin*, 1992; *Schweich et al.*, 1993]. With cation exchange as the dominant chemical reaction, one expects that during fresh-

ening of an aquifer the ions that are displaced from the saltwater exchange complex become spatially separated. Upstream of the saltwater-freshwater boundary, a sequence of Na^+, Mg^{2+}, and Ca^{2+} dominated water types should be found. This sequence has been observed in a field experiment by *Valocchi et al.* [1981], and it can be reproduced on a much smaller scale in a laboratory column [*Beekman and Appelo*, 1990]. We must therefore be confident that these chromatographic patterns are real and can be found in aquifers which are subjected to desalinization through some (natural) hydrogeological process.

However, the patterns are not so obvious that the characteristic sequence has been recognized and described in the hydrological literature beyond the observation that Ca/Na exchange takes place. For example, *Chapelle and Knobel* [1983] have described water quality patterns along freshening flow lines in the Aquia aquifer which exhibit the chromatographic sequence fairly closely, but they attribute relative increases of Mg^{2+} to reactions of solid carbonates and do not discuss the downstream peaking of K^+ concentrations. For the Lincolnshire limestone in England, *Lawrence et al.* [1976] and *Edmunds and Walton* [1983] found the characteristic freshening $NaHCO_3$ water quality and also observed a relative increase of Mg^{2+} downstream from the Na-dominated water, which is the wrong side for a chromatographic sequence. *Bishop and Lloyd* [1990] collected more data from the same aquifer and found a relative increase of Mg^{2+} and Sr^{2+} upstream from Na^+, but they still explained the Mg^{2+} increase using only solid carbonate reactions. In recent Dutch studies [*Beekman*, 1991; *Stuyfzand*, 1993] the patterns were sought more explicitly and have in fact been found to exist.

However, the clarity of the patterns on a regional aquifer scale is less ideal than that observed in field injections or laboratory studies. The clarity is a function of the ratio of adsorbed versus solute concentrations and also depends on whether sharp or broadening fronts develop. Chromatography will thus be more conspicuous when fresh water displaces saltwater than in the reverse situation, but dispersion and side reactions such as calcite dissolution (or precipitation) must be considered, as these may blur the patterns to such extent that the bands are smeared out and made unrecognizable. A geochemical transport model (PHREEQM) has been developed to account for these effects and will be used here to calculate freshening patterns in aquifers with parameters that are realistic for field conditions. The results demonstrate the importance of chromatographic effects on water quality in aquifers.

The structure of this paper is as follows. First, a description is given of the numerical background to the transport part of PHREEQM and of the model adopted for calculating cation and proton exchange. An example calculation for displacement of Na^+ and K^+ from a column by Ca^{2+} is compared with the analytical formulae using flushing factors. Subsequently, a laboratory experiment is described in which brackish water is displaced by freshwater to demonstrate that the chromatographic effects also exist in sandy aquifers with relatively low cation exchange capacity (CEC). These two examples are useful for explaining basic chromatographic features such as separation based on affinity sequences, and the effect of changes in salinity on solution composition. The model is then used to calculate chromatographic patterns in aquifers, discussing the importance of proton buffering and the effects of carbonate reactions. The last part of the paper is devoted to hydrogeochemical modeling of the most ideal pattern for a freshening aquifer that has been described in the literature: the Aquia aquifer in Maryland [Chapelle and Knobel, 1983].

The Geochemical Transport Model PHREEQM

PHREEQM is a one-dimensional transport model which uses the geochemical code PHREEQE [Parkhurst et al., 1980] to calculate geochemical reactions such as mineral-gas equilibrations, cation exchange, etc. The transport calculations are based on the mixing cell concept of Appelo and Willemsen [1987], which is essentially a finite difference solution (forward in time, central in space for dispersion, backward for advection) of the advection-dispersion-reaction equation:

$$\partial c/\partial t = -v\, \partial c/\partial x + D_L\, \partial^2 c/\partial x^2 - \partial q/\partial t \qquad (1)$$

where c is concentration in water (moles per liter), t is time (seconds), v is pore water flow velocity (meters per second), x is distance (meters), D_L is the hydrodynamic dispersion coefficient (squared meters per second; $D_L = D_f + \alpha_L v$, where D_f is the diffusion coefficient and α_L the dispersivity (meters)), and q is concentration in the solid phase (expressed as moles per liter of pore water).

Numerical dispersion is minimized by having always

$$(\Delta t)_A = \Delta x/v \qquad (2)$$

where $(\Delta t)_A$ is the time step for advective transport, and Δx is the cell length.

Numerical instabilities (oscillations) in the calculation of diffusion/dispersion are eliminated by having

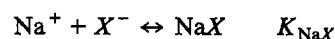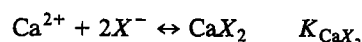$$(\Delta t)_D \le (\Delta x)^2/(3 D_L) \qquad (3)$$

where $(\Delta t)_D$ is the time step for dispersive/diffusive transport calculations. A properly constructed mixing cell model is stable as it fulfills the Courant condition for advective transport (equation (2)) and a Von Neumann criterion for dispersive transport calculations ((3); compare Press et al. [1989]). There are restrictions to grid and time size when both conditions must be satisfied, and small grid size may be precluded in the original version of the mixing cell model because of (3) [Dance and Reardon, 1983], or when field dispersion is mimicked by taking $(\Delta t)_A$ smaller than $\Delta x/v$ [Van Ommen, 1985], rather than by mixing of adjacent cells. In PHREEQM, smaller time steps for diffusive/dispersive transport than for advective transport are used, if necessary, and the grid can become as detailed as is needed to reduce numerical dispersion. Thus when (3) requires $(\Delta t)_D$ to be smaller than $(\Delta t)_A$, the conflict is solved by time stepping of diffusive transport until $\Sigma(\Delta t)_D = (\Delta t)_A$. Numerical dispersion is normally negligible when $\Delta x \le \alpha_L$, i.e., when $3(\Delta t)_D \le (\Delta t)_A$. After each time step, diffusive as well as advective, a call to PHREEQE is made to obtain the distribution of ions over pore water and solid, to dissolve or precipitate solids, to exchange solutes and adsorbed ions, and to add reactants; in short, to obtain $\partial q/\partial t$ in (1). In PHREEQE it is assumed that chemical equilibrium exists in and among all the phases. The explicit calculation is necessary because relations among solute and adsorbed ions may be strongly nonlinear. The program has been extensively tested and applied by Appelo et al. [1990], Postma et al. [1991], Glynn et al. [1991], and Griffioen [1993].

Ion Exchange in PHREEQM

Ion exchange reactions are modeled as ion association reactions in PHREEQM in the form of half reactions [Shaviv and Mattigod, 1985; Appelo and Willemsen, 1987; Viani and Bruton, 1992]. For example, for Na-Ca exchange the reaction

$$1/2 Ca^{2+} + Na\text{-}X \leftrightarrow 1/2 Ca\text{-}X_2 + Na^+ \qquad K_{Ca\backslash Na}$$
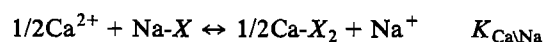
is split in two half reactions

$$Ca^{2+} + 2X^- \leftrightarrow CaX_2 \qquad K_{CaX_2}$$

$$Na^+ + X^- \leftrightarrow NaX \qquad K_{NaX}$$

which can be subtracted to provide the full exchange equation. Here, X^- represents the exchanger surface, and NaX and CaX_2 are the exchangeable cations which are calculated as association complexes. The half reactions are included in the database of PHREEQE using association constants relative to K_{NaX}. In the example, the value of $K_{CaX_2} = (K_{Ca\backslash Na} \cdot K_{NaX})^2$, where $K_{Ca\backslash Na}$ is derived from experiment.

Two problems must be resolved when cation exchange is modeled in this way. The first is that "free" X^- does not exist in a pure exchange model, since all X^- is neutralized by cations. This problem is circumvented when the association constants are high, since the concentration of free X^- then reduces essentially to zero; it is realized with $K_{NaX} \ge$

10^{20}. The second problem is that PHREEQE calculates activities of complexes such as NaX, CaX$_2$, etc., relative to the aqueous standard state of 1 mol/kg H$_2$O, whereas the activity of exchangeable cations is expressed as a fraction of exchange capacity. This problem is solved by calculating an equivalent fraction of the exchange capacity (Gaines and Thomas, [1953] convention) from the PHREEQE complex:

$$\beta_I = (i/\text{CEC})c_{IX_i}$$

where β_I is the equivalent fraction on the exchanger surface, i is the charge of cation I^{i+}, CEC is the cation exchange capacity (equivalents per kilogram H$_2$O), and c_{IX_i} is the complex concentration (moles per kilogram H$_2$O).

Activity Coefficients for Exchangeable Species

In heterovalent binary systems, where exchangeable cations have been determined for total solute concentrations that vary more than an order of magnitude [Wiklander, 1957; Van der Molen, 1958; Garcia-Miragaya and Page, 1976], the calculated exchange coefficient is more constant when activity coefficient corrections for solute ions are not applied. This is also valid for binary coefficients calculated in multicomponent systems [Van der Molen, 1958; Neal and Cooper, 1983]. These observations imply that for exchangeable cations a type of activity correction similar to the Debye Hückel theory may apply [cf. Neal and Cooper, 1983], because the major cations primarily reside as an outer sphere complex on the exchanging surfaces, i.e., while still hydrated. In the present version of PHREEQM, the exchanger composition is therefore calculated with activities of the free, uncomplexed aqueous cations. Activity coefficients for the exchangeable cations (the complexes IX_i) are equal to those in solution ($\gamma_{I^{i+}} = \gamma_{IX_i}$), unless noted otherwise.

Proton Exchange

Proton exchange can be incorporated similar to cations. However, it is well known that the loss of protons follows only gradually as pH increases [e.g., Davis and Kent, 1990; Stumm, 1992]. In other words, the acid dissociation constant for the reaction

$$\text{H-X} \leftrightarrow \text{H}^+ + X^-$$

is

$$K_a = \frac{[\text{H}^+][X^-]}{[\text{H-X}]}$$

where the apparent K_a is not a constant, but is decreasing as [H-X] decreases. The effect can be ascribed to an increase of the surface potential with increasing dissociation of surface groups that reduces the activity of adsorbed protons [Sposito, 1984; Stumm, 1992]. This results in

$$\log K_a = \log K_{int} + F\psi_0/(RT \ln 10) \qquad (4)$$

where K_{int} is the intrinsic dissociation constant at zero potential, F is the Faraday constant, ψ_0 is the potential at the surface where H$^+$ resides, R is the gas constant, and T is the absolute temperature. The constant capacitance model of Schindler and Stumm [1987] offers a method to relate the variation in K_a to other parameters. In the constant capacitance model, the surface potential is proportional to the deprotonated surface sites:

$$\psi_0 = -F\{X^-\}/\kappa\varepsilon \qquad (5)$$

where $\{X^-\}$ is the concentration of deprotonated surface sites (moles per square meter), and $\kappa\varepsilon$ is the specific capacitance. Combination of (4) and (5) gives

$$\log K_a = \log K_{int} - (F^2/(\kappa\varepsilon RT \ln 10))\{X^-\} \qquad (6)$$

The parameters before $\{X^-\}$ are customarily lumped as a factor α, and we may assume that $\{X^-\}$ is proportional to the fraction $f = (1 - \beta_H)$ that has dissociated, where β_H is the equivalent fraction of H-X of total X. This leads to

$$\log K_a = \log K_{int} - \alpha f \qquad (7a)$$

or

$$pK_a = pK_{int} + \alpha f \qquad (7b)$$

where p indicates $-\log$.

This equation adequately describes the linear increase of pK_a with $f > 0.3$ that is observed in titrations of solutions of fulvic acid (Marinsky [1987], $\alpha = 3.1$; Ephraim et al. [1989], $\alpha = 3.7$) and of humic acid (Tipping et al., [1988], $\alpha = 3.7$).

The change of pK_a has been included as an activity correction in PHREEQM, i.e.,

$$K_a = \frac{[\text{H}^+][X^-]}{[\text{HX}]} = \frac{[\text{H}^+][X^-]}{\phi_{HX}\beta_H}$$

where ϕ_{HX} is the activity coefficient for adsorbed H$^+$. Based on the modified constant capacitance model $\phi_{HX} = 10^{-\alpha(1-\beta_H)}$, where $\alpha = 3.4$ is an average from the quoted experiments with organic matter. The activity coefficient for the exchangeable proton thus decreases when the fraction of sites occupied by H$^+$ decreases, and the model relates exchangeable activity to "active fraction" which can be calculated by iteration. The exponential control of the H-X exchangeable fraction on the dissociation constant has, in practice, a great similarity to the way Tipping et al. [1988] include surface potential in their model for protonation of humic acids.

The model parameters are obtained by fitting to experimental data for the pH-dependent occupation of the soil exchange complex by base cations. Van der Molen [1958] and Pratt et al. [1962], among others, have shown that the apparent CEC for base cations of diverse soils may decrease by more than 2 as pH decreases from 8 to 5. Figure 1 shows this decrease for CaCO$_3$-free soils from the Netherlands [Van der Molen, 1958]. The solid line in Figure 1 is calculated using the active fraction model for 3-mM Ca(HCO$_3$)$_2$ solution as an average for the field conditions, with an α for H-X of 3.4 as for organic acids, and a log $K_{Ca\backslash H} = -2.1$ that is obtained for a change of β_H of 0.5 from pH = 5.038 to 8.038 ($c_{H^+} = 10^{-5}$ to 10^{-8} mol/L). It is interesting to note that the increase of exchangeable base cations with pH in the low pH range is determined solely by the factor α, which indicates that α for organic matter and the field soils is similar.

In the constant capacitance model the value for α depends on the concentration of the background electrolyte, a dependence that must be determined by separate experiments. An increase of the background electrolyte invariably shows up in a lower pK_a, i.e., the apparent dissociation of the surface H-X groups has increased. This increased dissociation can
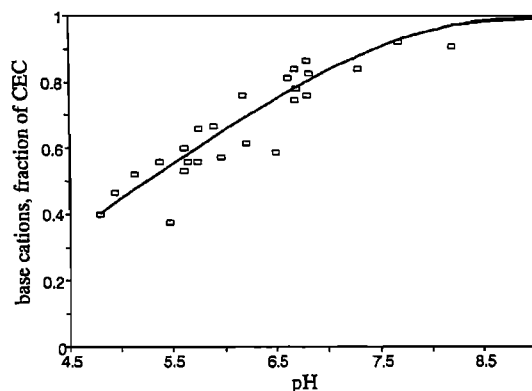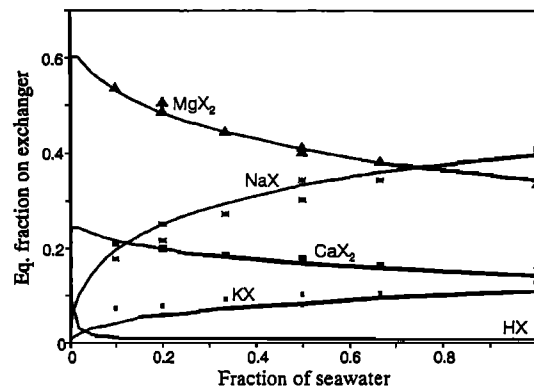
Figure 1. Percentage of base cations of CEC in Dutch soils as a function of pH. Data points are from *Van der Molen* [1958]. Line shows proton exchange with an exponential activity correction for [H-X]; compare text.

Figure 2. Fractions of exchangeable cations in mixtures of seawater and distilled water. Analyzed fractions [from *Van der Molen*, 1958] are indicated by single points; lines show the modeled composition using exchange coefficients from Table 1.

be ascribed to ion exchange of cations from the background electrolyte with protons on the surface and this line of thought is followed in PHREEQM. Other cations are thus coordinated via association reactions with X^- to make the exchanger electrically neutral. Electroneutrality is in fact necessary in a transport model, since the moving solution should also remain electrically neutral.

Summary of the Exchange Model

The activity correction for H-X can be extended to other adsorbed ions, allowing for a variable α for each ion to fit experimental data. This model implies a range for the exchange coefficient of two cations (in a binary mixture) that is equal to 10, powered with the sum of α for individual ions (i.e., the variation in $\log K_{IJ}$ becomes $\alpha_I + \alpha_J$). For our purpose it is important to relate the differences in exchange coefficients for the cations between saltwater and fresh water and correct only if necessary. The seawater exchange complex has been determined for numerous soils in the Netherlands, and the average β_I is given in Table 1 [*Van der Molen*, 1958]. Exchange coefficients $K_{I\backslash Na}$ for this composition were calculated in relation to the free ions in seawater obtained with PHREEQE and are also indicated in Table 1. The selectivities of the cations with respect to Na$^+$ are slightly on the high side compared to average (freshwater) values of $K_{I\backslash Na}$ as given in Table 1.

The differences in $\log K_{I\backslash Na}$ in seawater and in fresh water for the base cations are 0.2 for Mg^{2+} and Ca^{2+} and 0.4 for

K$^+$. An activity coefficient for Na-X has been used to model the low selectivity in seawater of the form $\log \phi_{NaX} = -0.5(1 - \beta_{Na})$ and $\log K_{NaX} = -0.5$, so that in fresh water with $\beta_{Na} \cong 0$, $\log K_{NaX} = 0$, while in seawater with $\beta_{Na} = 0.4$, the $\log K_{NaX} = -0.2$. It should be noted that the deviation is within the range observed for pure minerals and soils [*Bruggenwert and Kamphorst*, 1982] and may be compared to the range of saturation indexes (SI) (SI = $\log$ IAP/K) that is observed even for minerals such as calcite (SI = 0.7 for surface seawater). This may justify omitting activity corrections for ion exchange if the calculations are made for a natural system in which precise analytical data are not available. It is perhaps redundant to emphasize that this statement is not valid for protons, since α for H-X is much larger and indeed exerts quite an influence.

However, the model may improve the precision of calculations for base cations. Exchangeable cations have been computed for seawater diluted with distilled water and are compared in Figure 2 with analytical results given by *Van der Molen* [1958]. Where two points are plotted for a single fraction of seawater, these refer to two different soils that were used by Van der Molen. One soil (3 data points) is virtually free of CaCO$_3$ and has 8.1% organic matter and 27.4% clay <2 μm, whereas the other soil (used for all waters) has 7.0% CaCO$_3$, 3.6% organic matter, and 38.9% clay <2 μm. The exchange behavior of the two soils is similar, despite large differences in the basic properties of

Table 1. Exchange Parameters for Cations and Protons for Seawater and Freshwater

	Na$^+$	K$^+$	Mg^{2+}	Ca^{2+}	H$^+$
Experimental β_I (dimensionless)	0.399	0.109	0.344	0.142	0.005*
Free ion in seawater (M)	0.4788	0.0104	0.0487	0.0094	8.07 × 10^{-9}
Observed $\log K_{I\backslash Na}$	0	1.10	0.507	0.665	5.883*
Average $\log K_{I\backslash Na}$†	0	0.7	0.3	0.4	
Model $\log K_{IX}$‡	$-0.5 + 0.5 (1 - \beta_{Na})$	0.902	0.307	0.465	2.5 + 3.4 (1 − β_H)*

Note that $K_{I\backslash Na}$ for Mg^{2+} and Ca^{2+} are given for the reaction $1/2I^{2+}$ + Na-X ↔ $1/2I$-X_2 + Na$^+$.
*The parameters for H$^+$ have been obtained for average organic matter and Dutch soils as discussed in the text; β_H is calculated using these parameters.
†Freshwater average [compare *Bruggenwert and Kamphorst*, 1982].
‡To all $\log K_{IX}$, 20.0 is added in PHREEQM.

the material. The lines on Figure 2 indicate the calculated exchangeable cations, and these approach the analyzed fractions reasonably well.

Numerical Calculation of Chromatographic Patterns

A Test Example: Na^+ and K^+ are Flushed by Ca^{2+}

A simple system is the flushing of Na^+ and K^+ from an exchanger column with Ca^{2+} solution, and this may serve to illustrate chromatography as calculated with PHREEQM. Consider an exchanger with CEC = 1.1 meq/L and a 5 times higher (constant) selectivity for K^+ than for Na^+. A pore solution with $Na^+ = 1.0$ and $K^+ = 0.2$ mmol/L provides an exchanger composition with a ratio $\beta_{Na}/\beta_K = 1.0$. The column is flushed with 0.6 mmol/L $CaCl_2$, and the modeled outflow pattern for a column Peclet number of 40 is shown in Figure 3. The chromatographic pattern can be understood in terms of mass balances for adsorbed and solute ions. Initially, the effluent is in equilibrium with the original exchanger composition which yields a Na^+/K^+ ratio in solution of 5. The Na^+/K^+ ratio on the exchanger is 1, and therefore Na^+ is exhausted earlier than K^+. When Na^+ is flushed, K^+ increases in concentration to balance the anions. When this ion has also been removed from the column, Ca^{2+} finally appears. The fronts have a sharpening tendency because the K^+/Na^+ and Ca^{2+}/K^+ isotherms show a preference for the displacing ion: smaller concentrations of the displacing ion are retarded more.

The position of sharpening fronts can be calculated using simple mass balance over the front, with neglect of dispersion [Appelo et al., 1993]. In the column with pore volume V_0 (liters), the difference Δq_I (millimoles per liter) of exchangeable I^{i+} over a front is $V_0 \Delta q_I$ (millimoles). This quantity must be removed (or introduced) by a difference in solute concentration Δc_I (millimoles per liter). When this concentration difference is invariant for some time, a mass balance gives the volume V of incoming solution needed for flushing:

$$V = V_0 \Delta q_I / \Delta c_I$$

A sharp front flushing factor V^s can be defined which translates the volume V into column pore volumes:

$$V^s = V/V_0 = \Delta q_I / \Delta c_I$$

Thus in the given example, the first front occurs after complete loss of Na^+ from the exchanger:

$$V_1^s = \frac{(q_{Na})_1 - (q_{Na})_2}{(c_{Na})_1 - (c_{Na})_2} = \frac{0.55 - 0}{1.0 - 0} = 0.55$$

where q_{Na} is exchangeable Na^+ (millimoles per liter), c_{Na} is solute Na^+ (millimoles per liter), the subscript numerals indicate concentrations at the two sides of the front, and V_1^s is the number of pore volumes that must flush the column after the conservative front. Alternatively, the position of this front can be calculated from the change in K^+ concentration:

$$V_1^s = \frac{(q_K)_1 - (q_K)_2}{(c_K)_1 - (c_K)_2} = \frac{0.55 - 1.1}{0.2 - 1.2} = 0.55$$

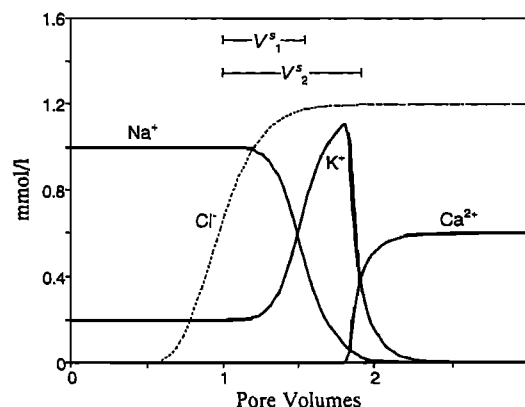**Figure 3.** A column with Na^+ and K^+ on the exchange complex is eluted with a $CaCl_2$ solution. PHREEQM model calculations compared with flushing factors V^s for the two sharp fronts. The Cl^- breakthrough coincides exactly with the analytical solution for an unretarded ion.

The second front follows from complete flushing of K^+:

$$V_2^s = \frac{(q_K)_2 - (q_K)_3}{(c_K)_2 - (c_K)_3} = \frac{1.1 - 0}{1.2 - 0} = 0.917$$

or, alternatively, from the arrival of Ca^{2+}:

$$V_2^s = \frac{(q_{Ca})_2 - (q_{Ca})_3}{(c_{Ca})_2 - (c_{Ca})_3} = \frac{0 - 0.55}{0 - 0.6} = 0.917$$

The calculated fronts are indicated in Figure 3. The crossover point of two ions from the numerical model falls slightly before the analytical front position because of tailing due to dispersion.

A Column Experiment

The chromatographic formulae applied in the preceding example have been given in dimensionless pore volumes of a column or flow line, and must be valid for field and laboratory alike. A simple experiment similar to the field injection described by *Valocchi et al.* [1981] was performed to show that the theory also applies in sandy aquifers with a low CEC. The aquifer described by Valocchi et al. has a CEC of 750 meq/L, whereas sandy aquifers have a CEC about 10 times lower.

Procedures and experimental design are described by *Appelo et al.* [1990]. Briefly, a sandy, anaerobic sediment from a Holocene channel fill in the Netherlands was cored and conserved in the field using liquid nitrogen. A 71-mm slice was cut from the core and was installed, while still frozen, in a laboratory column mounted in a 10°C water bath. Anaerobic solutions were pumped through the column with a LKB 2150 pump and were sampled at the outlet with a Gilson 220 fraction collector. First, native water and exchangeable cations were displaced with 25 mmol/L $SrCl_2$ to obtain CEC and exchange coefficients, and thereafter a freshwater injection in a brackish aquifer was simulated. The sediment was equilibrated with Cl-salt solution of Na^+, Mg^{2+}, and Ca^{2+} at a concentration of approximately 5 times diluted seawater, and flushed with fresh water that contained the three cations. Composition of the solutions, exchange coefficients, and physical conditions for the experiment are

Table 2. Solution Concentrations, Exchange Coefficients, and Flow Parameters for the Experiment and Model Shown in Figures 4 and 5

	Na^+	Mg^{2+}	Ca^{2+}	Cl^-
Initial	110.0	5.0	0.966	121
Injected	1.05	0.99	3.17	9.37
Log $K_{\Lambda Na}$	$-0.444 + 1.25\,(1 - \beta_{Na})$	0.219	0.397	

All values are given in millimoles per liter; CEC = 75 meq/L; column length = 71 mm; and α_L = 13 mm. There were 15 cells in the model.

summarized in Table 2. Note that the exchange coefficients are specific to the sediment and are slightly different from the average values given in Table 1.

Results of the freshening experiment are presented in Figure 4. A conspicuous decrease of Ca^{2+} and Mg^{2+} concentrations occurs initially. The concentrations are even lower than those in the injected water, and electroneutrality is maintained by a relative increase of the Na^+ concentration. Then Na^+ falls to the concentration in injected water, and the Mg^{2+} concentration peaks while Ca^{2+} still remains low. Finally, Mg^{2+} and Ca^{2+} level off to the concentrations in the injection fluid. The stages correspond to the earlier described sequence for the first example with an additional salinity front.

First, the dilution of pore water that is in equilibrium with brackish water creates a relative increase of Na^+ over the divalent ions in solution. The concentrations after such a salinity front can be calculated assuming that the exchanger (initially) has not changed from salt water equilibrium. Then, according to the law of mass action, the ratio

$$R_{I/Na} = \frac{c_I}{(c_{Na})^i} = \frac{\beta_I}{(\beta_{Na})^i}\,(K_{Na\backslash I})^i \qquad (8a)$$

is also constant for all ions I^{i+} which take part in the exchange reaction. Electroneutrality in solution gives the additional equation that can be used to calculate c_{Na} and, subsequently, from backsubstitution, c_I:
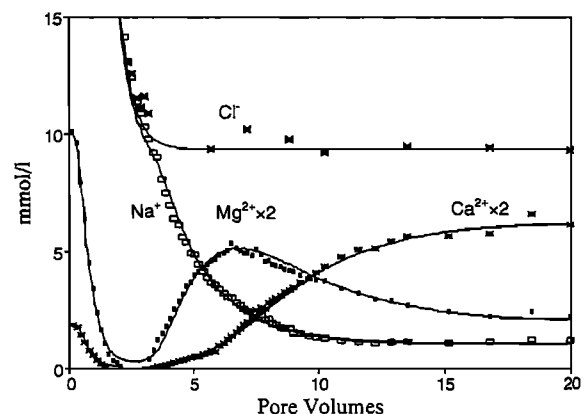
$$c_{Na} + \Sigma\, i c_I = N \qquad (8b)$$
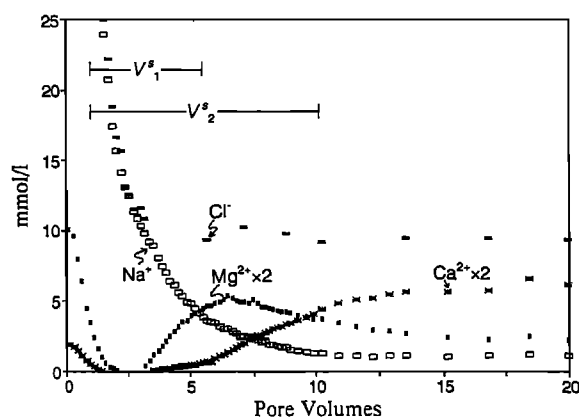
where N is the total concentration of cations in equivalents per liter.

Thus in the experiment, initial $R_{Mg/Na}$ = 0.413 and $R_{Ca/Na}$ = 0.08, which together with N = 9.37 × 10^{-3} eq/L (from Cl^- concentration when one pore volume has been flushed) yield c_{Na} = 9.28 mmol/L, c_{Mg} = 35.6 μmol/L, and c_{Ca} = 6.9 μmol/L. It will be noted that according to (8a) the ratio of homovalent ions does not change due to salinity effects, whereas the ratio of I^{2+}/Na^+ decreases 10^2 for a tenfold dilution of Na^+.

The column experiment illustrates that very low concentrations of Ca^{2+} and Mg^{2+} are indeed attained as salinity decreases (below detection limit in the fivefold diluted samples from the fraction collector). The anion charge is almost completely compensated by Na^+. This stage continues until Na^+ has been flushed from the exchange complex, which in this sediment is fairly rapid because the exchange capacity is small (base cation CEC = 75.1 meq/L pore water, and Na-X is initially 37.8 meq/L). After removal of Na-X, Mg^{2+} takes over, and when this ion has been exhausted the final injection water composition is approached. For three ions, as in this experiment, there are three compositions separated by two sharp fronts: first, the diluted solution in equilibrium with the initial exchange complex, second, an intermediate composition, and third, the injected water. These compositions are termed plateaux in chromatographic terminology [*Helfferich and Klein*, 1970].

The analytical solution for this displacement provides sharp front flushing factors V_1^s = 4.55 and V_2^s = 9.15 pore volumes, calculated using the formulae given by *Appelo et al.* [1993]. The front locations correspond (Figure 4) and only show a slight displacement that is related to the influence of dispersion in the experiment.

The results have also been simulated with PHREEQM, using a value for the dispersivity obtained by fitting the breakthrough of Cl^- with CXTFIT [*Parker and Van Genuchten*, 1984] and exchange coefficients given in Table 2. The results are presented in Figure 5. Exchange constants from experiment were used initially, without applying activity corrections for the exchangeable species. This leads to a quite steep decline of Na^+ and a similarly steep rise in Mg^{2+}, whereas the experiment shows tailing for elution of Na^+ and an early rise in Mg^{2+}. The introduction of an activity coefficient for Na-X can provide a better description

Figure 4. Elution of saline water from a sandy sediment in a column experiment. The initial Na^+ and Cl^- concentrations, 110 and 121 mmol/L, respectively, are not shown. Bars indicate the flushing factors for the two fronts.

Figure 5. PHREEQM modeling of the saltwater displacement shown in Figure 4.

Table 3. Initial Seawater and Freshwater Composition Used in Model Calculations

	pH	Na^+	K^+	Mg^{2+}	Ca^{2+}	Cl^-	HCO_3^-	SO_4^{2-}
Seawater	7.386	485.	10.6	55.1	10.66	566.	2.41	29.26
Freshwater	6.863	2.4	0.05	0.28	3.04	2.83	5.98	0.15

Concentrations are given in millimoles per kilogram H_2O.

of the observed data. The value $\alpha_{NaX} = 1.25$ was determined by fitting the tailing of Na^+, and the value for the association constant is then set by the amount of Na^+ that leaves the column. The presence of stagnant zones could be an alternative cause for the tailing of Na^+, but it has not been modeled. Most important is to note that the observed quality patterns are as predicted, both for a field scale experiment in an aquifer with a high cation exchange capacity [*Valocchi et al.*, 1981], and for a laboratory column containing sediment with a low exchange capacity typical for sandy material.

Proton adsorption was considered insignificant when the experiment was performed, but calculations with the proton exchange model suggest that $\beta_H = 0.135$ in the saltwater, and increases to $\beta_H = 0.155$ when in equilibrium with the injected water. The model results presented in Figure 5 are for calculations without H-X, but the model was also run to account for theoretical proton exchange. The simulation was made with CEC multiplied by $(1 - \beta_H)^{-1}$, and $K_{Mg\backslash Na}$ and $K_{Ca\backslash Na}$ also multiplied by $(1 - \beta_H)^{-1}$ to compensate for changes in β of these ions. An average $\beta_H = 0.145$ of initial and final water provided almost exactly the same results as given in Figure 5. This indicates that the column calculations are not greatly disturbed by neglecting H-X, as long as pH changes are small and salt concentrations do not importantly influence the concentrations of H-X.
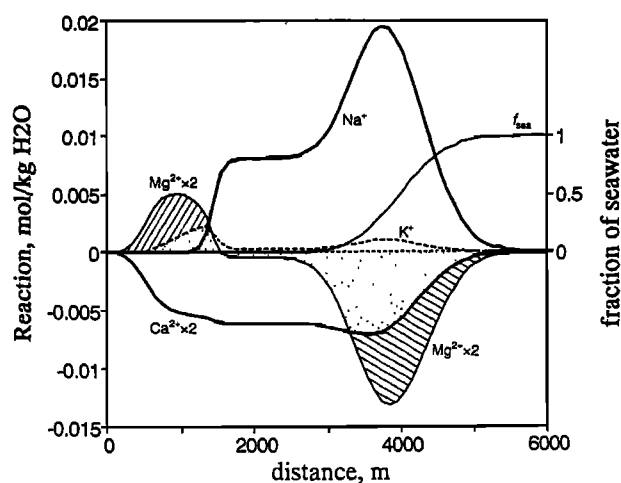
Figure 6. Cation exchange along a flow line when fresh water has displaced 4 km of seawater. The difference between model (solute) concentrations and a conservative mixture is plotted. Note the part of the flow line where Ca^{2+} displaces Mg^{2+}, additional to the zone where Ca^{2+} and Mg^{2+} displace Na^+.

Modeled Patterns Along an Aquifer Flow Line

Chromatographic patterns may become obscured in aquifers because boundary conditions are less uniform, dispersion is larger, flow patterns are variable, and flow directions may even reverse, and because other chemical reactions take place in addition to, or are even triggered by the exchange reactions. The effects can be illustrated with example calculations for the situation where seawater is displaced by fresh water. The two boundary water types are given in Table 3, and exchange coefficients are as noted in Table 1. Seawater was equilibrated with calcite and used as the water quality that resides initially in the aquifer which has CEC = 50 meq/kg H_2O. This was flushed by fresh water, a mixture of 99.5% 3 mM $Ca(HCO_3)_2$, and 0.5% seawater with the pH of equilibrium with calcite. Water temperature was 25°C throughout these simulations. The grid comprised 65 cells of 100 m, with a dispersivity of 33 m; for the first 3300 m also a finer grid with 33 m cells was used. Displacement of seawater by fresh water, with only cation and proton exchange as chemical reactions, is illustrated in Figure 6. Absolute concentration changes have been plotted, calculated from the difference of the model concentration and the concentration in a conservative mixture of the two end compositions:

$$c_{I,react} = c_{I,model} - c_{I,mix}$$

where $c_{I,model}$ is the model concentration of ion I^{i+}, $c_{I,mix}$ is the conservative concentration in the mixture calculated from the Cl^- concentration, and $c_{I,react}$ indicates the absolute change due to reactions.

The chromatographic separation of the cations is again clear in Figure 6 and follows the imposed selectivity order: first, Na^+ is eluted (compensated by uptake of Ca^{2+} and Mg^{2+}), then K^+ (compensated by Ca^{2+}), and last Mg^{2+} (also replaced by Ca^{2+}). The parts where Mg^{2+} is involved in the exchange reaction have been hatched in Figure 6 (and dotted where coinciding with the reaction of another ion) to show that there is a section of the flowline where Mg^{2+} joins Ca^{2+} in displacing Na^+, but also a part where Ca^{2+} displaces Mg^{2+}. The combination of uptake and release is not normally considered in mass balance calculations on cation exchange along an aquifer flow line, although it obviously can be significant.

From the freshwater-seawater boundary upstream there is a dilution plateau in which Na^+ and K^+ increase, while Ca^{2+} and Mg^{2+} decrease due to the lower salinity while the exchanger composition has not yet altered significantly. The exchange of Na^+ is enhanced in the mixing zone because total concentrations are higher. The effect can be calculated from the theoretical concentration of Na^+ in equilibrium with an exchanger of fixed composition and with infinite capacity (equations (8a) and (8b)):
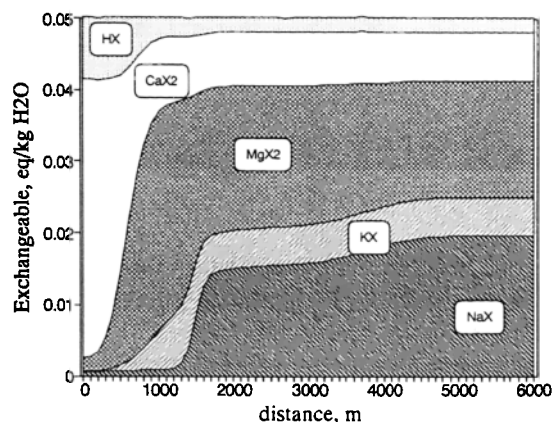
Figure 7. Composition of exchange complex along a flow line when seawater is displaced by fresh water (compare Figure 6).

$$c_{Na} = \{-(1 + R_{K/Na}) + [(1 + R_{K/Na})^2 + 8(R_{Mg/Na}$$

$$+ R_{Ca/Na})N]^{1/2}\}[4(R_{Mg/Na} + R_{Ca/Na})]^{-1} \quad (8c)$$

where $R_{I/Na}$ indicates, as before, the concentration ratio (moles per liter) of ion I^{i+} over $(Na^+)^i$ in the displaced water (seawater in this case), and N is the total cation concentration in equivalents per liter in the displacing solution. It follows from mass balance that the enlarged loss of Na^+ in the mixing zone reduces the lateral extent of Na^+ dominated water because Na^+ is exhausted earlier. The increase is accompanied by uptake of Mg^{2+} on the exchanger, which will later on lengthen the flushing stage of Mg^{2+}. The net effect of mixing on the total time length of exchange is in this case therefore almost nil.

The composition of the exchange complex along the flow line is given in Figure 7. Figure 7 further demonstrates that in the mixing zone a loss of Na-X occurs, which is compensated by a gain of Mg-X_2, while the other ions are not affected. Figure 7 also shows that after depletion of Na-X, a decrease of K-X takes place, then an increase of H-X and, last, a decrease of Mg-X_2. In total, there are four fronts after the freshwater-seawater boundary, and the concentrations of all ions change over each front, both in the exchanger and in solution.

Proton buffering occurs in two intervals along the flow line, one where the major increase of H-X takes place before Mg-X_2 decreases, and the other in the dilution plateau. The buffering is conspicuous in the trend of pH along the flow line shown in Figure 8. From $pH = 6.86$ in the injected fluid, the value increases to 7.9–8, and then on to 8.8 in the Na^+ dominated water quality, to decrease again to the value of calcite equilibrated seawater in the mixing zone. The high pH in Na^+ dominated water is due simply to the exchanger buffer, which tries to maintain the ratio c_H/c_{Na} equal to the seawater ratio when salinity decreases. The proton buffering is clearly manifest in the alkalinity changes along the flow line (Figure 8). TIC in Figure 8 is a conservative parameter because reactions with solid carbonates do not take place, and exchange of anions has not been considered. The increase of alkalinity with pH is due to the reactions
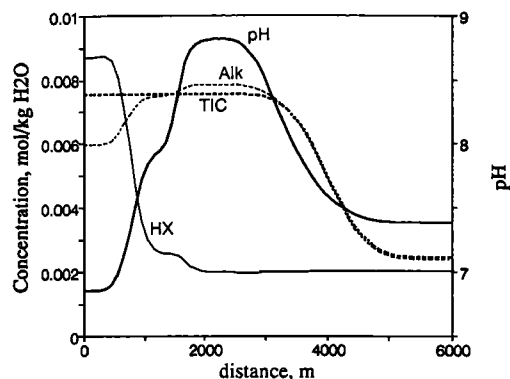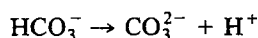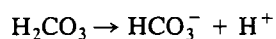
$$H_2CO_3 \rightarrow HCO_3^- + H^+$$

$$HCO_3^- \rightarrow CO_3^{2-} + H^+$$

Figure 8. Effects of proton buffering on pH, alkalinity (equivalents per kilogram H_2O), and TIC along a flow line when seawater is displaced by fresh water (compare Figure 6).

They are the source of protons needed for the increase of H-X in the freshening flow line.

Proton buffering, in combination with Ca^{2+} and alkalinity variations, will trigger calcite dissolution or precipitation. A second run for the same water qualities but with calcite equilibrium imposed in addition illustrates the complex patterns which arise. Figure 9 shows total amounts of calcite dissolved (plus) or precipitated (minus) when the freshwater front has arrived at 4 km. The behavior along the flow line can be explained in terms of earlier discussed exchange reactions. From the freshwater-saltwater boundary in an upstream direction, one can observe calcite precipitation due to an increase of pH in the mixing zone. Further upstream in the Na^+ dominated water, where Ca^{2+} concentrations are very low, more calcite has dissolved than was precipitated during the earlier passage of the freshwater-saltwater mixing zone. Still further upstream where H-X increases, the loss of protons from solution has again caused precipitation of calcite. Last, at the upstream end, the loss of Ca^{2+} from solution (exchanging for Mg^{2+}) causes calcite to dissolve; this is also the net result of the overall reaction.

An interesting point is that the proton buffering that can be present in clayey intercalations in limestone, or in marls, would prevent Mischungskorrosion [cf. *Sanford and Konikow*, 1989] in the case of a freshening aquifer. In a salinizing
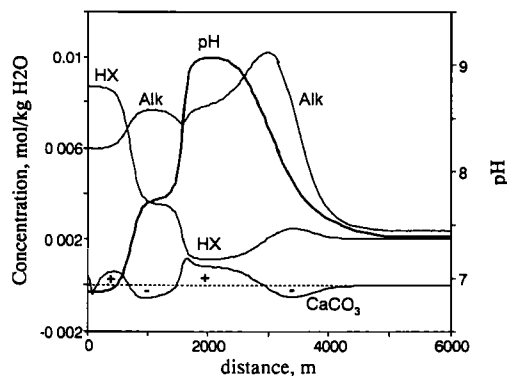

Figure 9. Carbonate reactions along a flow line; seawater displaced by fresh water (compare Figure 6) with calcite equilibrium imposed.
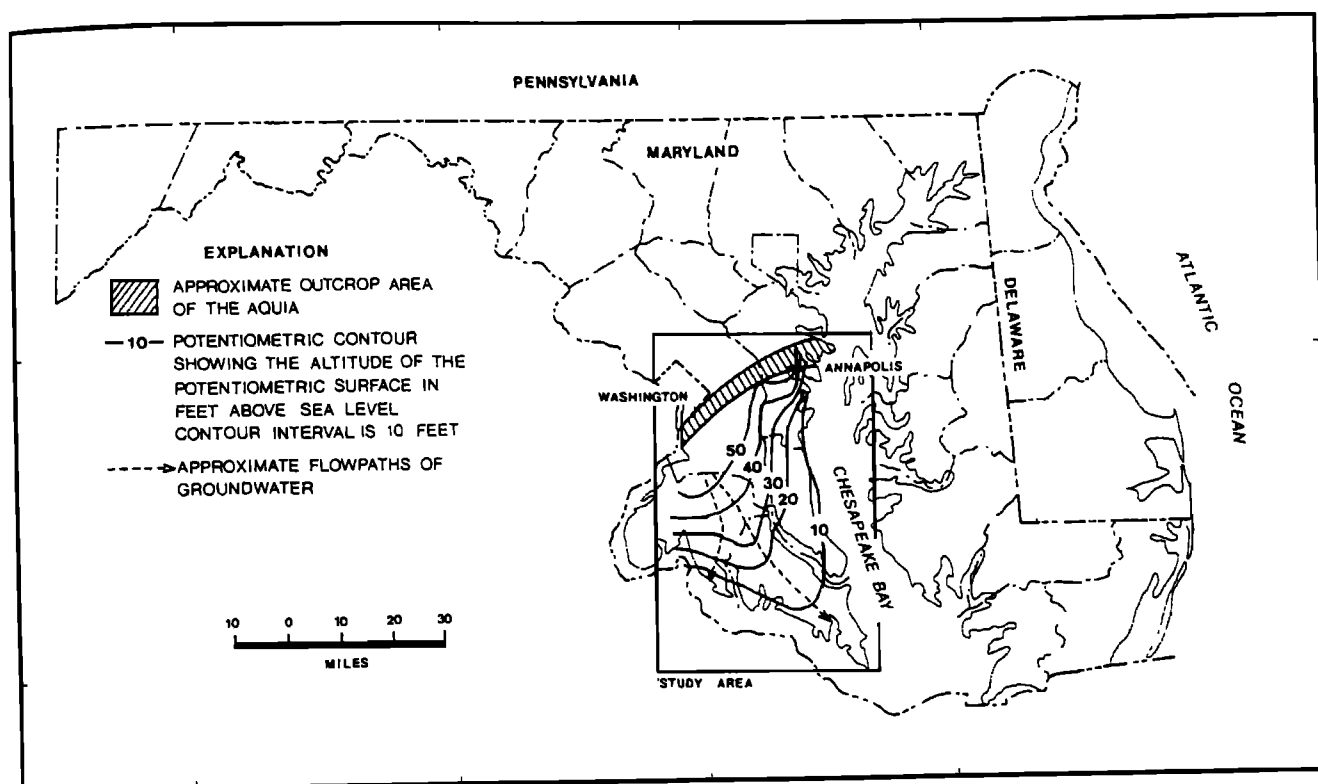
Figure 10. Outline of the Aquia aquifer in Maryland with estimated prepumping head distribution [*Chapelle and Knobel*, 1983]. (1 foot equals 0.3046 m; 1 mile equals 1.608 km.) Reproduced with permission from *Ground Water*.

aquifer, however, the pH will decrease as a result of salinity increase, and proton exchange will then enhance the dissolution tendency of the mixed water. Also, in a freshening aquifer, Ca-X_2 will have increased more than H-X has decreased after final equilibration with freshwater, which means that cation exchange finally generates more calcite dissolution than in its absence. The overall pattern of solute and exchanging cations does not change much from the former case without calcite.

Modeling of Water Qualities in the Aquia Aquifer

NaHCO$_3$ type water in coastal plain aquifers of the eastern United States has been related to freshening of the aquifer [*Foster*, 1950; *Back*, 1966; *Chapelle*, 1983; *Chapelle and Knobel*, 1983]. Probably the most complete picture of a freshening aquifer has been presented by *Chapelle and Knobel* [1983] when depicting major cation patterns as a function of flow length in the Aquia aquifer. The water quality in this aquifer shows zonal bands with changes in concentrations of the major cations that have been attributed, besides cation exchange which releases Na$^+$ into solution, to dissolution of Mg calcites, and precipitation of pure calcite [*Chapelle*, 1983]. The pattern is, on the other hand, similar to what can be expected for a chromatographic pattern in which Mg^{2+} is released at a later stage than Na$^+$. The flow line in the Aquia aquifer even exhibits a band where K$^+$ concentrations are high at the expected position in the chromatographic sequence.

The observed water quality pattern has been modeled with PHREEQM modified for the specific hydraulic conditions of the Aquia aquifer. The aim was to determine whether the

water quality could be described assuming simple and acceptable paleohydrological conditions.

Hydraulic and Hydrochemical Boundary Conditions

The estimated prepumping head distribution in the aquifer is shown in Figure 10 [*Chapelle and Knobel*, 1983], and Figure 11 shows a schematic cross section along a flow path. The aquifer is bounded to the east by a change in facies [*Chapelle and Drummond*, 1983]. The prepumping hydraulic head distribution suggests a confined aquifer in the upstream half and gradual loss of water in the downstream part of the aquifer. Leakage probably occurs via Pleistocene channels which cut through the confining beds [*Chapelle and Drummond*, 1983]. The hydrological conditions have been modeled assuming a one-dimensional flow tube with recharge at $x = 0$, and with seepage into the confining layers evenly distributed over the second half of the flow tube. In practice, this means that in PHREEQM each cell in the second half of the flow tube transmits only a fraction into its neighbor cell, the remainder being lost. In the adapted code, the transferred fraction F is

$$F_{n \to n+1} = 2 - 2n/\text{NCOL} \qquad n > \text{NCOL}/2$$

where n is the cell number counting from the recharge end, and NCOL is the total number of cells in the grid.

It was assumed that the initial water quality was brackish as a result of mixing of seawater with fresh water during deposition of the overlying Marlboro clay, which is a brackish water clay. The Na$^+$/K$^+$/Mg^{2+} ratios in the initial water are taken equal to seawater. The dilution in the palaeo aquifer can then be estimated from the Na$^+$/Mg^{2+} ratio in the NaHCO$_3$ water now observed, using (8), in which N is
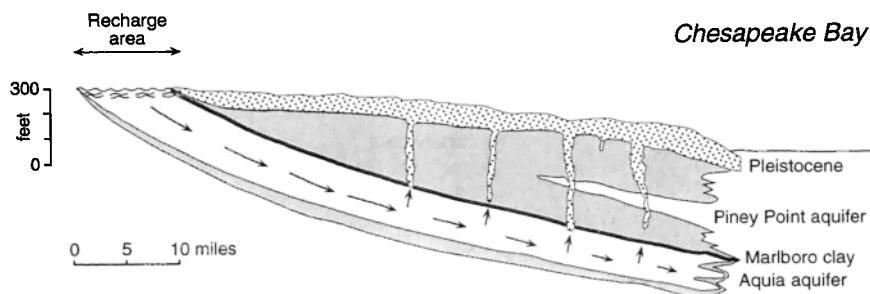
Figure 11. Schematic cross section of the Aquia aquifer. Recharge occurs in the outcrop of the formation; discharge is schematized to take place evenly in the downstream half. (1 foot equals 0.3046 m; 1 mile equals 1.608 km.)

known (sum of the cations in the resident water quality) but in which the ratio $R_{Mg/Na} = c_{Mg}/(c_{Na})^2$, and also of the other ions varies as a function of the dilution. In the waters from four wells (FE 1, FE 21, FF 21, FF 35; *Drummond* [1984]) with more than 4 mmol/L Na^+, the average $c_{Na} = 5.3$ mmol/L, and the Na^+/Mg^{2+} molar ratio is 77, which indicates that the original formation water is only 18% seawater. In practice, there are disturbing effects through initial uptake of Mg^{2+} in the mixing zone (compare Figure 6), dissolution of calcite, the limited sediment exchange capacity, and also effects arising from solute complexes. However, the choice for 18% seawater determines the relative amounts of exchangeable Na^+, K^+, and Mg^{2+} (compare Figure 2) and is therefore checked by the final fit that can be obtained. The other 82% is assumed to be 3 mM $Ca(HCO_3)_2$ water; this also fixes the Cl^- concentration.

The anions HCO_3^- and SO_4^{2-} are determined by additional conditions. It was observed doing the simulations that in the initial aquifer, exchangeable H-X had to be at least equal to exchangeable Na-X to obtain sufficient proton buffering to maintain the pH below the maximum of 9.0 observed in the aquifer. This means that the original 18% seawater must have had a pH below 7. A low pH may be related to SO_4^{2-} reduction and equivalent replacement with HCO_3^-, and was realized by reducing 5 mmol/L SO_4^{2-}; the pH was adapted to obtain equilibrium with calcite at 15°C.

The recharge water quality is presumed to be unchanged from that analyzed in the upstream reaches of the aquifer. In the recharge area, acid waters with low ion concentrations are present, which indicate that the aquifer has become decalcified in parts. Furthermore, a large variation in alkalinity is present in the initial reach, which levels off to 2.8 meq/L after 15 miles (1 mile = 1.6 km) down the average flow path. With a pH of 7.5, this alkalinity translates to a CO_2 pressure of $10^{-2.4}$ atm, which is low for open system dissolution of calcite at a temperature of 15°C [*Harmon et al.*, 1975], but may be related to calcite dissolution in the recharge area under partly open, partly closed conditions with respect to CO_2. Decalcification may have developed over time, and original equilibration of recharge water with calcite in the soil zone would have given greater alkalinity in the past. The assumed constant water quality for the model has the leveled off alkalinity, obtained by dissolution of pure calcite, 0.1 mmol/L Na^+ and Cl^-, and 0.05 mmol/L K^+ as observed in the recharge area.

Exchange Parameters

The aquifer contains 10–35% glauconite as the major cation exchanger [*Chapelle and Knobel*, 1983]. Glauconite is

an illite type clay mineral that contains significant amounts of Fe^{2+} and Fe^{3+} but otherwise behaves in the same manner as illite with respect to exchange capacity and selectivity [*Davydov and Levitskii*, 1950; *Vanderdeelen*, 1964; *Kolosova et al.*, 1971]. For Aquia glauconite, *Chapelle and Knobel* [1983] have found an extremely high selectivity for K^+ and also a fairly high selectivity for Na^+, which did not yield the observed chromatographic pattern of water qualities when used in the model calculations. Other determinations of exchange coefficients for glauconite do not indicate such an extremely high specificity for K^+. *Kolosova et al.* [1971] give $K_{K\backslash Na} = 9.1$ and 11.9 for two glauconites with a different origin. *Vanderdeelen* [1964] determined distribution coefficients for Sr^{2+} and Li^+ on glauconite in Ca-K-H systems, and using the data in the ternary system a $K_{Ca\backslash K} = 0.44$ is obtained. Furthermore, from Sr distribution coefficients in the binary systems (i.e., either K or Ca glauconite with traces of Sr^{2+}), $K_{Sr\backslash Ca} = 1.30$ and $K_{Sr\backslash K} = 0.56$ is calculated, which also give $K_{Ca\backslash K} = 0.43$. These coefficients are normal for illite-type clay minerals [*Bruggenwert and Kamphorst*, 1982] and are similar to the exchange coefficients noted in Table 1 for Dutch soils that have illite as the dominant clay mineral. The exchange coefficients from Table 1 were therefore used in further calculations. The exchange capacity for the aquifer sediment was estimated for 33% glauconite with an average exchange capacity of 10 meq/100 g and a bulk density over porosity factor of 6 kg/L. This produces an exchange capacity of 200 meq/L pore water.

It is of interest to note that *Vanderdeelen* [1964] also determined distribution coefficients for H glauconite, prepared at pH < 2.0. However, experimental difficulties were recorded and exchange coefficients cannot be calculated. At more neutral pH a substantial proton exchange capacity was observed as well, but since the pH of the final equilibrium solution is unknown, a selectivity for H-X cannot be calculated. During model calculations it was found that the intrinsic pK_{int} noted in Table 1 for H-X had to be increased to 3.0 to provide sufficient H-X to counterbalance Na-X, and thus obtain pH values comparable to those from the field.

Fine Tuning

In the last phase of the modeling exercise, the dispersivity in the upper part of the aquifer was optimized by trial and error to 2.0 miles (3.2 km), while in the downstream zone where the confining beds are leaky, dispersion was limited to the fractional transfer of cell contents. Finally, to obtain recharge water quality in the first 10 miles (16 km) of the flow path, the exchange capacity for the first 10 miles was set to zero. The observed chromatographic peaks were matched

Table 4. Hydrochemical Conditions for Modeling the Quality Patterns in the Aquia Aquifer

	pH	Na^+	K^+	Mg^{2+}	Ca^{2+}	Cl^-	HCO_3^-	SO_4^{2-}	X^-
Initial	6.80	87.4	1.9	9.92	4.38	101.8	15.5	0.27	200
Recharge	7.57	0.1	0.05	0.0	1.40	0.1	2.8	0.0	

Concentrations are given in millimoles per kilogram H_2O. Other parameters of the model were as follows: 20 cells of 3.2 miles (5.1 km); a dispersivity of 2.0 miles (3.2 km) in the upstream reach, and calcite equilibrium throughout.

by model results when the total pore volume of the upstream half of the aquifer was flushed 8.0 times. The hydrochemical conditions for the model are summarized in Table 4.

Model Results

The model fit shown in Figure 12 for the major cations and alkalinity is quite satisfactory, but this type of modeling contains arbitrary aspects. Nevertheless, some features were relatively insensitive to the model parameters, and these may denote the more global value of the exercise. First, it is again noted that the sequential appearance of Mg^{2+} and K^+ is specific to the chromatographic separation and can be varied in the model only by varying the Mg^{2+}/K^+

Figure 12. Concentrations of Na^+, alkalinity (milliequivalents per liter), K^+, Mg^{2+}, Ca^{2+}, and pH along a flow path in the Aquia aquifer (Maryland). Data points are from *Chapelle and Knobel* [1983]; lines are modeled concentrations using PHREEQM.

selectivity. Second, an apparent dip in alkalinity is observed just before the start of the $NaHCO_3$ water quality, which is matched by the model. This localized decrease in alkalinity is always found for the cases where proton exchange is incorporated in the model, and is due to the changes in H-X over that front in combination with the precipitation of calcite (compare also Figure 9). Third, the upstream increase of Ca^{2+} concentrations in the parts where K^+ and Mg^{2+} are peaking indicates an increased concentration of Ca-X_2. The increase occurred during flushing of Na^+ and is due to dissolution of large amounts of calcite. Fourth, the increase of Na^+ and alkalinity at the downstream end is universal in the model calculations, and in agreement with earlier conclusions about the development of $NaHCO_3$ water quality in a freshening aquifer [*Foster*, 1950; *Back*, 1966; *Chapelle and Knobel*, 1983]. However, to keep pH below 9.0 as observed in aquifers, a source of acid is necessary.

The relatively low pH indicates that the reaction is not simply

$$H_2O + CaCO_3 + 2Na\text{-}X \rightarrow Ca\text{-}X_2$$

$$+ 2Na^+ + HCO_3^- + OH^- \qquad (9)$$
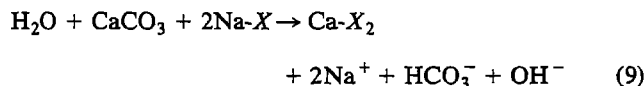
since OH^- (or CO_3^{2-} that results from $HCO_3^- + OH^- \rightarrow CO_3^{2-} + H_2O$) does not contribute significantly to alkalinity at a pH below 9.0. The low pH has been modeled with Fe^{2+} ion exchange/hydroxide mass transfers [*Plummer et al.*, 1991], but the usual explanation is sought in an additional source of CO_2 which takes away the OH^- produced in reaction (9):

$$CO_2 + OH^- \rightarrow HCO_3^-$$
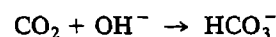
The CO_2 could be derived from organic matter via methane/ CO_2 digestion [*Foster*, 1950] or via reduction of SO_4^{2-} that diffuses from the confining beds [*Chapelle and McMahon*, 1991].

The proton exchange model offers an alternative explanation via the reaction

$$CaCO_3 + Na\text{-}X + H\text{-}X \rightarrow Ca\text{-}X_2 + Na^+ + HCO_3^-$$
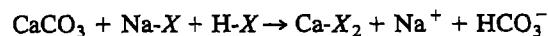
and it is of interest to reconsider here the mass balance calculations in which $\delta^{13}C$ has been employed as control for the reaction scheme [*Chapelle and Knobel*, 1985]. In the upstream part of the Aquia aquifer, where alkalinity is about 2.8 meq/L, $\delta^{13}C$ of TIC is approximately $-13\%o$, which is expected if half of the TIC originates from CO_2 gas with $\delta^{13}C \approx -26\%o$, and the other half is derived from calcite with $\delta^{13}C \approx 0\%o$. In $NaHCO_3$ water with about 5 meq/L alkalinity, $\delta^{13}C$ is $-6\%o$. A reaction scheme which involves a source of CO_2 from organic matter invariably leads to values of $\delta^{13}C$ in $NaHCO_3$ water that are too low, but can be explained if large amounts of aragonite recrystallize into calcite [*McMahon and Chapelle*, 1991; *Plummer et al.*, 1991]. Proton exchange is another very simple mechanism to
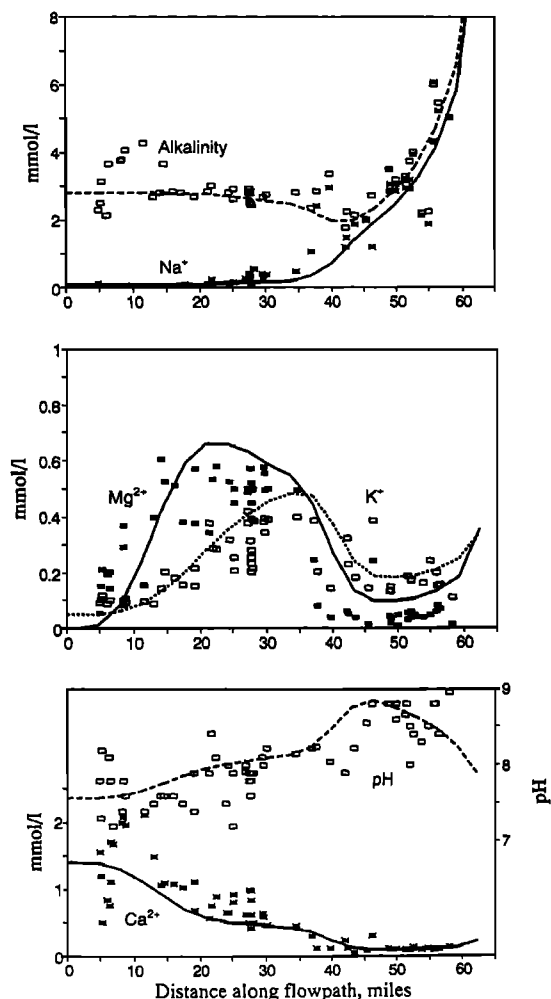
provide pH buffering, and at the same time it can readily explain the $\delta^{13}C$ value observed in $NaHCO_3$ water, since calcite with $\delta^{13}C \approx 0‰$ is the only source of the approximately doubled alkalinity and TIC.

The match of calculated and observed chromatographic pattern provides paleohydrological information about the Aquia system. The upper 32 miles (51.5 km) of the aquifer must have been flushed 8.0 times under the model conditions. With a porosity of approximately 0.3, this means that 76.8 miles (124 km) of water must have entered the aquifer and flushed the saltwater, and part of the saltwater cations from the exchange complex. *Purdy et al.* [1992] estimate an age of approximately 12 ka for a point at 29 miles (46.7 km) in the flow path, so that the now observed chromatographic pattern in the aquifer could have been established in 100 ka. This falls far short of the Paleocene age of the Aquia sediments and may indicate that either flow velocities have been much smaller in the past, or that freshening started late during the Quaternary.

Summary and Conclusions

The chromatographic separation of ions during displacement of different water types in aquifers has been demonstrated for the case of freshwater displacement. In this case the displacing cation is usually Ca^{2+}, which has a higher affinity for the exchanger than the displaced saltwater ions Na^+, K^+, and Mg^{2+} and produces sharpening fronts that can be calculated with simple mass balance formulae. An important aspect is that given equilibrium with seawater, appreciable amounts of Mg^{2+} and K^+ are adsorbed on the exchanger in addition to Na^+. These ions must also be flushed during freshening. An ordered sequence develops for the cations, whereby first Na^+, then K^+, and finally Mg^{2+} is displaced. The theoretical patterns have been modeled numerically with proton exchange included in a form derived from the constant capacitance model of *Schindler and Stumm* [1987]. Model calculations show that H-X is the last of the monovalent cations to exchange owing to its high affinity. Proton exchange is important for calcite reactions. Model calculations predict that calcite can precipitate in the mixing zone of fresh water and seawater because the c_H/c_{Na} ratio in solution is initially buffered by the exchange complex. A decreasing salinity is therefore automatically accompanied by increase of pH, which may induce the precipitation of calcite. Conversely, an increasing salinity is related to a decrease of pH in the mixing zone, and this will enhance calcite dissolution. These effects may be important in marly aquifers which have sufficient exchange capacity and exchangeable protons available for buffering. The overall patterns for a freshening aquifer are remarkably uniform and are not particularly dependent on additional reactions that are triggered by cation exchange. Disturbances from the ideal model are more likely to be caused by dispersion, reversals of flow patterns, and uneven distribution of initial water qualities.

However, the patterns have been found in the Aquia aquifer in Maryland. The observed water chemistry displays the expected sequential peaks of Mg^{2+}, K^+, and Na^+ and could be modeled with satisfactory precision. This is considered the best proof that ion exchange in aquifers is more comprehensive than Ca^{2+} for Na^+, or Mg^{2+} for Na^+ exchange. It was shown that the Aquia aquifer also displays

Ca^{2+} for K^+ and Ca^{2+} for Mg^{2+} exchange. Proton exchange in $NaHCO_3$ type water is an important factor, which can easily explain observed $\delta^{13}C$ values in the aquifer. A major conclusion therefore is that chromatographic patterns should be considered as one of the common features of groundwater chemistry, as important and widespread as carbonate reactions. The principal difference is that carbonate reactions normally occur in steady state and become dynamic only when a mineral is exhausted. Ion exchange reactions are always dynamic by their very nature and will give heterogeneous patterns of ion concentrations and side reactions along a flow line. Variable initial conditions along a flow line and varying flow in response to hydrogeological changes will blur the pattern and may make it unrecognizable, so that only the $NaHCO_3$ water quality remains as a conspicuous indicator. However, when it is present in its full development, the dynamic nature of ion exchange allows for a link with historic flow conditions and can be used to obtain paleohydrological information about the aquifer system. In the case of the Aquia aquifer it was deduced that the initial water quality before emergence of the sediments was not pure seawater. After emergence about 124 km (77 miles) of water have entered the aquifer, flushing the saltwater and the saltwater ions from the exchange complex over a period of approximately 100 ka.

References

Appelo, C. A. J., and A. Willemsen, Geochemical calculations and observations on salt water intrusions, 1, A combined geochemical/mixing cell model, *J. Hydrol.*, *94*, 313–330, 1987.

Appelo, C. A. J., A. Willemsen, H. E. Beekman, and J. Griffioen, Geochemical calculations and observations on salt water intrusions, 2, Validation of a geochemical model with column experiments, *J. Hydrol.*, *120*, 225–250, 1990.

Appelo, C. A. J., J. H. Hendriks, and M. van Veldhuizen, Flushing factors and a sharp front solution for solute transport with multicomponent ion exchange, *J. Hydrol.*, *146*, 89–113, 1993.

Back, W., Hydrochemical facies and groundwater flow patterns in northern part of Atlantic coastal plain, *U.S. Geol. Surv. Prof. Pap.*, *498-A*, 42 pp., 1966.

Beekman, H. E., Ion chromatography of fresh- and seawater intrusion, Ph.D. thesis, 198 pp., Free Univ., Amsterdam, 1991.

Beekman, H. E., and C. A. J. Appelo, Ion chromatography of fresh- and salt-water displacement: Laboratory experiments and multicomponent transport modelling, *J. Contam. Hydrol.*, *7*, 21–37, 1990.

Bishop, P. K., and J. W. Lloyd, Chemical and isotopic evidence for hydrogeochemical processes occurring in the Lincolnshire limestone, *J. Hydrol.*, *121*, 293–320, 1990.

Bruggenwert, M. G. M., and A. Kamphorst, Survey of experimental information on cation exchange in soil systems, in *Soil Chemistry*, B, *Physico-chemical Models*, edited by G. H. Bolt, pp. 141–203, Elsevier, New York, 1982.

Chapelle, F. H., Groundwater geochemistry and calcite cementation of the Aquia aquifer in southern Maryland, *Water Resour. Res.*, *19*, 545–558, 1983.

Chapelle, F. H., and D. D. Drummond, Hydrogeology, digital simulation, and geochemistry of the Aquia and Piney Point–Nanjemoy aquifer system in Southern Maryland, *Rep. Invest. 38*, Md. Geol. Surv., Baltimore, 1983.

Chapelle, F. H., and L. L. Knobel, Aqueous geochemistry and exchangeable cation composition of glauconite in the Aquia aquifer, Maryland, *Ground Water*, *21*, 343–352, 1983.

Chapelle, F. H., and L. L. Knobel, Stable carbon isotopes of HCO_3^- in the Aquia aquifer, Maryland: Evidence for an isotopically heavy source of CO_2, Ground Water, 23, 592–599, 1985.

Chapelle, F. H., and P. B. McMahon, Geochemistry of dissolved inorganic carbon in a coastal plain aquifer, 1, Sulfate from confining beds as an oxidant in microbial CO_2 production, J. Hydrol., 127, 85–108, 1991.

Charbeneau, R. J., Multicomponent exchange and subsurface transport: Characteristics, coherence, and the Riemann problem, Water Resour. Res., 24, 57–64, 1988.

Dance, J. T., and E. J. Reardon, Migration of contaminants in groundwater at a landfill: A case study, 5, Cation migration in the dispersion test, J. Hydrol., 63, 109–130, 1983.

Davis, J. A., and D. B. Kent, Surface complexation modeling in aqueous geochemistry, in Mineral-Water Interface Geochemistry, Rev. Mineral., vol. 23, edited by M. F. Hochella Jr. and A. F. White, pp. 177–260, Mineralogical Society of America, Washington, D. C., 1990.

Davydov, A. T., and I. Y. Levitskii, Adsorbed cations on glauconite (in Russian), Zh. Obsch. Khim., 20, 1776–1779, 1950.

Drummond, D. D., Records of selected wells, Calvert and St. Mary's counties, Maryland, Rep. 14, Md. Geol. Surv., Baltimore, 1984.

Edmunds, W. M., and N. R. G. Walton, The Lincolnshire limestone—Hydrogeochemical evolution over a ten-year period, J. Hydrol., 61, 201–211, 1983.

Ephraim, J. H., H. Borén, C. Pettersson, I. Arsenie, and B. Allard, A novel description of the acid-base properties of an aquatic fulvic acid, Environ. Sci. Technol., 23, 356–362, 1989.

Foster, M. D., The origin of high sodium bicarbonate waters in the Atlantic and Gulf coastal plains, Geochim. Cosmochim. Acta, 1, 33–48, 1950.

Friedly, J. C., and J. Rubin, Solute transport with multiple equilibrium-controlled or kinetically controlled chemical reactions, Water Resour. Res., 28, 1935–1953, 1992.

Gaines, G. L., and H. C. Thomas, Adsorption studies on clay minerals, II, A formulation of the thermodynamics of exchange adsorption, J. Chem. Phys., 21, 714–718, 1953.

Garcia-Miragaya, J., and A. L. Page, Influence of ionic strength and inorganic complex formation on the sorption of trace amounts of Cd by montmorillonite, Soil Sci. Soc. Am. J., 40, 658–663, 1976.

Glynn, P. D., P. Engesgaard, and K. L. Kipp, Two geochemical mass transport codes: PHREEQM and MST1D, their use and limitations at the Pinal Creek toxic waste site, U.S. Geol. Surv. Water Resour. Inv., 91-4034, 1991.

Griffioen, J., Multicomponent cation exchange including alkalinization/acidification following flow through sandy sediment, Water Resour. Res., 29, 3005–3019, 1993.

Harmon, R. S., W. B. White, J. J. Drake, and J. W. Hess, Regional hydrochemistry of North American carbonate terrains, Water Resour. Res., 11, 963–967, 1975.

Helfferich, F., and G. Klein, Multicomponent Chromatography, Marcel Dekker, New York, 1970.

Kolosova, G. M., V. A. Nikashina, M. N. Yakimova, I. B. Serova, and E. Y. Severinenko, Calculations for ion-exchange processes on glauconites, Russ. J. Phys. Chem., 45, 1466–1469, 1971.

Lawrence, A. R., J. W. Lloyd, and J. M. Marsh, Hydrochemistry and groundwater mixing in part of the Lincolnshire limestone aquifer, England, Ground Water, 14, 12–20, 1976.

Marinsky, J. A., A two-phase model for the interpretation of proton and metal ion interaction with charged polyelectrolyte gels and their linear analogs, in Aquatic Surface Chemistry, edited by W. Stumm, pp. 49–81, John Wiley, New York, 1987.

McMahon, P. B., and F. H. Chapelle, Geochemistry of dissolved inorganic carbon in a coastal plain aquifer, 2, Modeling carbon sources, sinks, and $\delta^{13}C$ evolution, J. Hydrol., 127, 109–135, 1991.

Neal, C., and D. M. Cooper, Extended version of Gouy-Chapman electrostatic theory as applied to the exchange behavior of clay in natural waters, Clays Clay Miner., 31, 367–376, 1983.

Parker, J. C., and M. T. Van Genuchten, Determining transport parameters from laboratory and field tracer experiments, Rep. 84-3, 96 pp., Va. Agric. Exp. Stat., Blacksburg, 1984.

Parkhurst, D. L., D. C. Thorstenson, and L. N. Plummer,

PHREEQE—A computer program for geochemical calculations, U.S. Geol. Surv. Water Resour. Invest., 80-96, 210 pp., 1980.

Plummer, L. N., E. C. Prestemon, and D. L. Parkhurst, An interactive code (NETPATH) for modeling net geochemical reactions along a flow path, U.S. Geol. Surv. Water Resour. Invest. Rep., 91-4078, 226 pp., 1991.

Pope, G. A., L. W. Lake, and F. G. Helfferich, Cation exchange in chemical flooding, 1, Basic theory without dispersion, Soc. Pet. Eng. J., 418–433, 1978.

Postma, D., C. Boesen, H. Kristiansen, and F. Larsen, Nitrate reduction in an unconfined sandy aquifer: Water chemistry, reduction processes and geochemical modeling, Water Resour. Res., 27, 2027–2045, 1991.

Pratt, P. F., L. D. Whittig, and B. L. Grover, Effect of pH on the sodium-calcium exchange equilibria in soils, Soil Sci. Soc. Am. Proc., 26, 227–230, 1962.

Press, W. H., B. P. Flannery, S. A. Teukolsky, and W. T. Vetterling, Numerical Recipes in Pascal, 759 pp., Cambridge University Press, New York, 1989.

Purdy, C. B., G. S. Burr, M. Rubin, G. R. Helz, and A. C. Mignerey, Dissolved organic and inorganic ^{14}C concentrations and ages for coastal plain aquifers in southern Maryland, Radiocarbon, 34, 654–663, 1992.

Sanford, W. E., and L. F. Konikow, Simulation of calcite dissolution and porosity changes in saltwater mixing zones in coastal aquifers, Water Resour. Res., 25, 655–667, 1989.

Schindler, P. W., and W. Stumm, The surface chemistry of oxides, hydroxides and oxide minerals, in Aquatic Surface Chemistry, edited by W. Stumm, pp. 83–110, John Wiley, New York, 1987.

Schweich, D., M. Sardin, and M. Jauzein, Properties of concentration waves in presence of nonlinear sorption, precipitation/dissolution, and homogeneous reactions, 1, Fundamentals, Water Resour. Res., 29, 723–733, 1993.

Shaviv, A., and S. V. Mattigod, Exchange equilibria in soils expressed as cation-ligand complex formation, Soil Sci. Soc. Am. J., 49, 569–573, 1985.

Sposito, G., The Surface Chemistry of Soils, 234 pp., Oxford University Press, New York, 1984.

Stumm, W., Chemistry of the Solid-Water Interface, 428 pp., John Wiley, New York, 1992.

Stuyfzand, P. J., Hydrochemistry and hydrology of the coastal dune area of the western Netherlands, Ph.D. thesis, 366 pp., Free Univ., Amsterdam, Netherlands, 1993.

Tipping, E., C. A. Backes, and M. A. Hurley, The complexation of protons, aluminum and calcium by aquatic humic substances: A model incorporating binding-site heterogeneity and macro-ionic effects, Water Res., 22, 597–611, 1988.

Valocchi, A. J., R. L. Street, and P. V. Roberts, Transport of ion-exchanging solutes in groundwater: Chromatographic theory and field simulation, Water Resour. Res., 17, 1517–1527, 1981.

Vanderdeelen, J., Equilibres physico-chimiques de radio-isotopes dans un système "sol-eau," Pedologie, 14, 24–35, 1964.

Van der Molen, W. H., The Exchangeable Cations in Soils Flooded with Sea Water, 167 pp., The Hague, Staatsdrukkerij, 1958.

Van Ommen, H. C., The mixing cell concept applied to transport of non-reactive and reactive components in soils and groundwater, J. Hydrol., 78, 201–213, 1985.

Viani, B. E., and C. J. Bruton, Modeling ion exchange in clinoptilolite using the EQ3/6 geochemical modeling code, Water-Rock Interaction, Proceedings of 7th Symposium, edited by Y. K. Kharaka and A. S. Maest, 73–77, A. A. Balkema, Rotterdam, Netherlands, 1992.

Walsh, M. P., S. L. Bryant, R. S. Schechter, and L. W. Lake, Precipitation and dissolution of solids attending flow through porous media, AIChE. J., 30, 317–328, 1984.

Wiklander, L., Cation and anion exchange phenomena, in Chemistry of the Soil, edited by F. E. Bear, pp. 107–148, Reinhold, New York, 1957.

C. A. J. Appelo, Faculty of Earth Sciences, Vrije Universiteit, De Boelelaan 1085, 1081 HV Amsterdam, Netherlands. (e-mail: appt@geo.vu.nl)